

# The Regulation of Glucose-Excited Neurons in the Hypothalamic Arcuate Nucleus by Glucose and Feeding-Relevant Peptides

R. Wang,<sup>1</sup> X. Liu,<sup>1</sup> S.T. Hentges,<sup>2</sup> A.A. Dunn-Meynell,<sup>3,4</sup> B.E. Levin,<sup>1,3,4</sup> W. Wang,<sup>1</sup> and V.H. Routh<sup>1,3</sup>

**Glucosensing neurons in the hypothalamic arcuate nucleus (ARC) were studied using electrophysiological and immunocytochemical techniques in neonatal male Sprague-Dawley rats. We identified glucose-excited and -inhibited neurons, which increase and decrease, respectively, their action potential frequency (APF) as extracellular glucose levels increase throughout the physiological range. Glucose-inhibited neurons were found predominantly in the medial ARC, whereas glucose-excited neurons were found in the lateral ARC. ARC glucose-excited neurons in brain slices dose-dependently increased their APF and decreased their ATP-sensitive K<sup>+</sup> channel (K<sub>ATP</sub> channel) currents as extracellular glucose levels increased from 0.1 to 10 mmol/l. However, glucose sensitivity was greatest as extracellular glucose decreased to <2.5 mmol/l. The glucokinase inhibitor alloxan increases K<sub>ATP</sub> single-channel currents in glucose-excited neurons in a manner similar to low glucose. Leptin did not alter the activity of ARC glucose-excited neurons. Although insulin did not affect ARC glucose-excited neurons in the presence of 2.5 mmol/l (steady-state) glucose, they were stimulated by insulin in the presence of 0.1 mmol/l glucose. Neuropeptide Y (NPY) inhibited and  $\alpha$ -melanocyte-stimulating hormone stimulated ARC glucose-excited neurons. ARC glucose-excited neurons did not show pro-opiomelanocortin immunoreactivity. These data suggest that ARC glucose-excited neurons may serve an integrative role in the regulation of energy balance. *Diabetes* 53:1959–1965, 2004**

From the <sup>1</sup>Department of Pharmacology and Physiology, New Jersey Medical School (UMDNJ), Newark, New Jersey; the <sup>2</sup>Oregon Health and Science University, Vollum Institute, Portland, Oregon; the <sup>3</sup>Department of Neurosciences, New Jersey Medical School (UMDNJ), Newark, New Jersey; and the <sup>4</sup>Neurology Service, Veterans Administration Medical Center, East Orange, New Jersey.

Address correspondence and reprint requests to Vanessa H. Routh, PhD, Department of Pharmacology and Physiology, New Jersey Medical School (UMDNJ), P.O. Box 1709, Newark, NJ 07101-1709. E-mail: routhvh@umdnj.edu.

Received for publication 6 February 2004 and accepted in revised form 23 April 2004.

W.W. is currently affiliated with Robert S. Dow Neurobiology Laboratories, Legacy Research, Portland, Oregon.

ACSF, artificial cerebrospinal fluid; APF, action potential frequency; ARC, arcuate nucleus; K<sub>ATP</sub> channel, ATP-sensitive K<sup>+</sup> channel;  $\alpha$ -MSH,  $\alpha$ -melanocyte-stimulating hormone; NPY, neuropeptide Y; POMC, proopiomelanocortin; PVN, paraventricular nucleus; VMH, ventromedial hypothalamus; VMN, ventromedial hypothalamic nucleus.

© 2004 by the American Diabetes Association.

**T**he hypothalamic arcuate nucleus (ARC) is in a pivotal position for involvement in the central control of glucose homeostasis. The ARC houses neuropeptide Y (NPY) and proopiomelanocortin (POMC) neurons, which have opposing effects on the regulation of food intake and energy balance. NPY neurons project to the hypothalamic paraventricular nucleus (PVN). This pathway favors anabolic processes, including increased food intake and decreased energy expenditure (1–3). In contrast, the ARC POMC neurons mediate catabolic processes (4). ARC NPY and POMC neurons receive input from central and peripheral metabolic signals involved in the regulation of food intake and energy balance (e.g., monoamines, insulin, and leptin) (1,2,5). Furthermore, they project to the sympathetic cell bodies in the spinal cord (6,7). The ARC also possesses glucosensing neurons (8,9). Thus, the ARC is a critical center for the integration and regulation of systems involved in the central control of energy homeostasis.

To date, there are few electrophysiological studies characterizing ARC glucosensing neurons (8,9). Moreover, these studies of ARC glucosensing neurons have been performed using nonphysiological levels of extracellular glucose. That is, ARC glucosensing neurons have been characterized by decreasing extracellular glucose from 10 or 20 to 0 mmol/l. An extracellular glucose level of 0 mmol/l is incompatible with life, and brain glucose levels may never exceed 5 mmol/l. Studies in anesthetized rats using a glucose oxidase electrode have shown that glucose levels in the ventromedial hypothalamus (VMH; which contains the ARC and the ventromedial hypothalamic nucleus [VMN]) vary from 0.2 to 4.5 mmol/l as plasma glucose levels increase from 2 to 18 mmol/l, with steady-state levels being ~2.5 mmol/l (10). A recent report using microdialysis (zero-net flux method) (11) in awake animals showed that VMH glucose levels decreased from 1.5 mmol/l in fed rats to 0.73 mmol/l after an overnight fast (12). Therefore, it is necessary to reevaluate and redefine the electrophysiological characteristics of purported ARC glucosensing neurons under more physiological conditions to determine their relevance to physiological glucose sensing. We have recently shown that VMN glucosensing neurons are sensitive to physiological levels of extracellular glucose (13). In this study we found two types of VMN neurons that respond directly to physiological changes in extracellular glucose. Glucose-excited neurons increase

and glucose-inhibited neurons decrease their action potential frequency (APF) as extracellular glucose levels increase from 0.1 to 2.5 mmol/l. Glucose-excited and -inhibited neurons express mRNA for the pancreatic form of glucokinase, the rate-limiting enzyme in glycolysis. Thus, glucokinase may confer the ability to sense glucose by allowing intracellular metabolism to fluctuate with extracellular glucose levels (14,15). Importantly, other VMN neurons alter their firing rate in response to a variety of extracellular glucose concentrations, but none of these neurons are inherently glucose sensing. Instead, the observed effects are due to presynaptic inputs from other glucosensing neurons whose cell bodies may reside outside the VMN. One location of these presynaptic glucose-sensing inputs to the VMN may be the ARC. Thus, in this study we determined whether ARC glucosensing neurons are able to sense changes in extracellular glucose within the physiological range. Furthermore, we tested the hypothesis that ARC glucosensing neurons play an integrative role in the regulation of energy homeostasis. To do this we determined whether they are sensitive to insulin and leptin as well as the feeding-relevant peptides NPY and  $\alpha$ -melanocyte-stimulating hormone ( $\alpha$ -MSH; the POMC cleavage product) (4).

## RESEARCH DESIGN AND METHODS

**Preparation of brain slices.** Male 14- to 21-day-old Sprague-Dawley rats were housed with their dams at 22–23°C on a 12-h light/dark cycle and given chow (Purina Rat Chow 5001) and water ad libitum. On the day of experiment, rats were anesthetized with ketamine/xylazine and transcardially perfused as described previously (13). Brains were rapidly removed and placed in ice-cold (slushy) oxygenated (95% O<sub>2</sub>:5% CO<sub>2</sub>) perfusion solution. Sections (350  $\mu$ m) through the hypothalamus were maintained at 34°C in oxygenated high-Mg<sup>2+</sup> low-Ca<sup>2+</sup> artificial cerebrospinal fluid (ACSF; in mmol/l: 127 NaCl, 1.9 KCl, 1.2 KH<sub>2</sub>PO<sub>4</sub>, 26 NaHCO<sub>3</sub>, 2.5 glucose, 9 MgCl<sub>2</sub>, and 0.3 CaCl<sub>2</sub>, osmolarity adjusted to ~300 mOsm with sucrose, pH 7.4) for 30 min and allowed to come to room temperature until use. Slices were then transferred to normal oxygenated ACSF (2.4 mmol/l CaCl<sub>2</sub> and 1.3 mmol/l MgCl<sub>2</sub>) for the remainder of the day. High-Mg<sup>2+</sup> ACSF solutions (3.1 mmol/l MgCl<sub>2</sub>:0.3 CaCl<sub>2</sub> or 11 mmol/l MgCl<sub>2</sub>:2.4 CaCl<sub>2</sub>) were used to block presynaptic input as described previously (13).

### Electrophysiology

**Whole-cell recordings in brain slices.** Immediately before use, brain slices were placed in a chamber (Warner Instruments) with the temperature controlled at 33–34°C. During recording, brain slices were perfused at 6 ml/min with normal oxygenated ACSF. Viable neurons were visualized and studied under infrared differential interference contrast microscopy as described previously (13). Current- and voltage-clamp recordings (standard and perforated patch whole-cell recording configuration) from neurons in the ARC were made using an Axopatch 1D amplifier (Axon Instruments), low pass-filtered at 1 kHz, and monitored using Axoscope software (Axon). Data were simultaneously digitized at 5 kHz (Digidata 1320A; Axon Instruments) and analyzed using pClamp9 software (Axon). The junction potential between the patch pipette and the bath solutions was nulled before the gigaohm seal formation. For standard whole-cell recording, borosilicate pipettes (1.5–3.5 M $\Omega$ ; Sutter Instruments) were filled with an intracellular solution containing the following (in mmol/l): 128 K-gluconate, 10 KCl, 10 KOH, 10 HEPES, 4 MgCl<sub>2</sub>, 0.05 CaCl<sub>2</sub>, 0.5 EGTA, 2 Na<sub>2</sub>ATP, and 2 lucifer yellow, pH 7.2, with osmolarity adjusted to 290–300 mOsm with sucrose. Only neurons with access resistance <15 M $\Omega$  were used. For perforated patch whole-cell recording, amphotericin was included in the patch pipette (final concentration 240  $\mu$ g/ml, stock 60 mg/ml DMSO). Membrane potential and APF were allowed to stabilize for 10–15 min after the formation of a gigaohm seal. Neurons whose access resistance exceeded 40 M $\Omega$  were rejected. After recording, the membrane was ruptured to allow lucifer yellow access into the cell for 5 min for future immunocytochemical labeling. No differences in glucose sensitivity were observed between standard and perforated patch recording configurations. Extracellular glucose and other chemicals (Sigma) were added to the ACSF perfusion solution as described in the figures. Input resistance was calculated from the change in membrane potential in response to small 500-ms hyperpolarizing pulses (–10 or –20 pA) given every 3 s as described

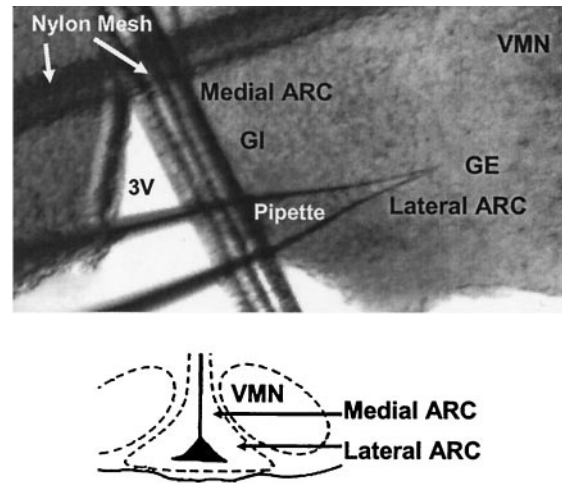


**FIG. 1.** Location of ARC glucose-excited and glucose-inhibited neurons. GE, glucose-excited; GI, glucose-inhibited.

previously. The reversal potential was calculated from the change in membrane current in response to voltage steps from –120 mV to +60 mV from a holding potential of –60 mV. Steady-state currents were determined by measuring data points within the last 5 ms of the 200-ms voltage pulses.

**Single-channel recording in cultured VMH neurons.** Brain slices were prepared as described above, and sections (400  $\mu$ m) were immediately transferred to zero-glucose/zero-pyruvate Hibernate media (Brain Bits) supplemented with 2% (vol/vol) B-27, 2.5 mmol/l glucose, 1 mmol/l L-lactate, 0.23 mmol/l pyruvate, 0.5 mmol/l L-glutamine, and 100 units/ml penicillin/streptomycin (Hibernate). The VMH was dissected and then digested in papain-containing media. Tissue was incubated for 30 min in a 30°C water bath with a platform rotating at 100 rpm and then rinsed and triturated. The cell suspension was centrifuged 4 min at room temperature at 1,000 rpm, and the pellet was resuspended with 1–1.5 ml zero-glucose/zero-pyruvate Neurobasal (Invitrogen) with 2% B27, 2.5 mmol/l glucose, 1 mmol/l L-lactate, 0.23 mmol/l pyruvate, 0.5 mmol/l L-glutamine, 100 units/ml penicillin/streptomycin, and 5 ng/ml bFGF2 (Neurobasal) (16). Cells were plated in Neurobasal on culture dishes and used within 4 days. Single ATP-sensitive K<sup>+</sup> channel (K<sub>ATP</sub> channel) currents were recorded and analyzed as described previously (17). Single-channel activity was quantified as the mean current (I) passed through the K<sub>ATP</sub> channel for 60-s segments of data, as follows:  $I = NP_o i$ , where  $N$  is the number of channels,  $P_o$  is the open probability, and  $i$  is the single channel current amplitude.

**Immunocytochemistry.** For immunocytochemistry, all solutions were prepared in 0.1 mol/l PBS, pH 7.4, with 0.2% triton X and used at room temperature, except where otherwise noted. After recording, slices were fixed in 4% paraformaldehyde (without triton X) then sunk in 4°C 30% sucrose (also without triton X). Tissue was frozen, subsectioned at 20  $\mu$ m and mounted on subbed slides. The slides were treated with 1% H<sub>2</sub>O<sub>2</sub> and then blocked in 10% normal donkey serum (Jackson Immunoresearch). After an overnight treatment in 10% donkey serum with 0.02% rabbit anti-POMC precursor (Phoenix Pharmaceuticals), slides were placed in 0.2% biotinylated goat anti-rabbit IgG (Vector Laboratories). Sections were then processed using an ABC kit (Vector Laboratories) followed (as previously described) (18) by a tyramide signal amplification system (Perkin Elmer) using CY3 visualization. To amplify the lucifer yellow label, slides were retreated with 1% H<sub>2</sub>O<sub>2</sub>, followed by an avidin and biotin blocking kit (Vector Laboratories). They were next placed in 10% normal horse serum (Jackson Immunoresearch) and then held overnight in 1:400 biotinylated rabbit anti-lucifer yellow (Molecular Probes). The ABC procedure, followed by tyramide signal amplification system, was performed as above, this time using fluorescein visualization. After final washing, sections were coverslipped with Vectashield (Vector Laboratories) and analyzed using fluorescence microscopy. Subsections were visualized using each laser channel sequentially as well as simultaneously to avoid bleed-through between channels.

## RESULTS

Electrophysiological and immunocytochemical techniques were used to characterize 421 ARC neurons with regard to their sensitivity to glucose, leptin, insulin, NPY, and  $\alpha$ -MSH. In recordings made throughout the entire ARC,

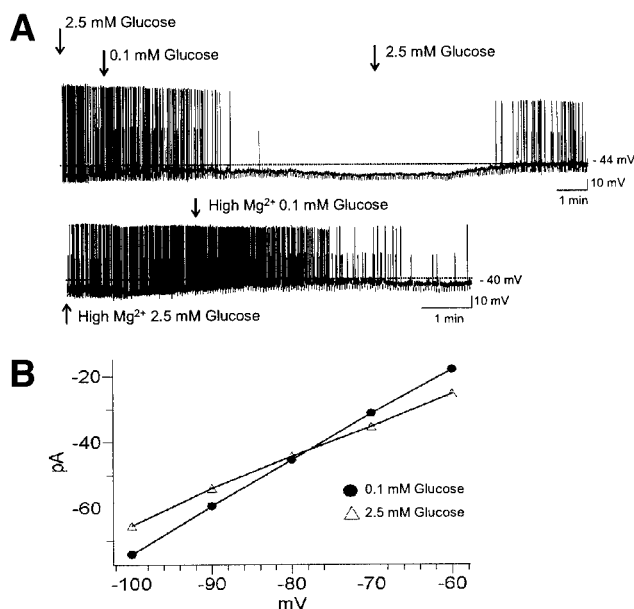


**FIG. 2. A:** Consecutive whole-cell current clamp recordings of spontaneous electrical activity in an ARC glucose-excited neuron. Resting membrane potential is indicated by the horizontal line and noted to the right of each trace in this and subsequent figures. Similarly, downward deflections represent the membrane voltage response to a constant hyperpolarizing pulse. Decreasing extracellular glucose levels from 2.5 to 0.1 mmol/l causes hyperpolarization, decreased APF, and decreased input resistance (*top trace*). This response persists in high-Mg<sup>2+</sup> solution (*bottom trace*). **B:** Voltage-current relations indicate that the glucose-sensitive conductance reverses at the theoretical K<sup>+</sup> equilibrium potential.

two types of intrinsically glucose-sensing neurons were found that were similar to the glucose-excited and glucose-inhibited neurons, which we have described previously in the VMN (13). These two subtypes of glucosensing neurons were unequally distributed between the medial and lateral ARC. When recordings were made predominantly in the medial ARC, 14% (12 of 83) of the neurons were of the glucose-inhibited subtype, whereas only 4% (3 of 83) were of the glucose-excited subtype. In contrast, when recordings were made in the lateral ARC, 13% (45 of 338) were of the glucose-excited subtype, and only 1% (3 of 338) were of the glucose-inhibited subtype (Fig. 1). The densest population of glucose-excited neurons was actually located on the lateral border of the ARC, near

the cell-poor region between the ARC and the VMN. This study focuses predominantly on the ARC glucose-excited neurons.

The general characteristics of ARC glucose-excited neurons are shown in Fig. 2. Glucose-excited neurons hyperpolarize their membrane potential and decrease their APF as extracellular glucose levels decrease. This is accompanied by a decrease in input resistance (Fig. 2A, *top trace*). The latency of the glucose response was  $5.6 \pm 0.3$  min ( $n = 38$ ). We believe that this is caused by the time required for diffusion of glucose through the brain slice, as well as the time required for glucose metabolism to raise intracellular ATP, alter K<sub>ATP</sub> channel activity, and finally decrease APF. The glucose response of glucose-excited neurons is intrinsic, as indicated by the persistence of this response in high-Mg<sup>2+</sup> ACSF, which abolishes presynaptic input ( $n = 12$ ) (Fig. 2A, *bottom trace*). Current-voltage relations show that the glucose-induced current reverses at  $-79 \pm 3$  mV ( $n = 27$ ), which is close to the theoretical K<sup>+</sup> equilibrium potential of  $-99$  mV in our solutions (Fig. 2B). This, together with the observation that the inhibitory effect of decreased glucose is reversed by the sulfonylurea tolbutamide (100  $\mu$ mol/l) (not shown), indicates that the K<sub>ATP</sub> channel is responsible for the glucose-induced current ( $n = 8$ ). Finally, decreasing extracellular glucose from 2.5 to 0.5 mmol/l or the presence of the glucokinase inhibitor alloxan (4 mmol/l) in 2.5 mmol/l glucose reversibly increases the K<sub>ATP</sub> channel current by  $222 \pm 115\%$  ( $n = 5$ ;  $P = 0.05$ , Students paired *t* test) in cultured VMH neurons (Fig. 3). The single-channel current that was induced by both alloxan and 0.5 mmol/l glucose was blocked by tolbutamide and had a conductance of  $\sim 46$  pS, as we have shown before for the K<sub>ATP</sub> channel in hypothalamic neurons (17).

We next addressed the question of whether ARC glucose-excited neurons are only sensitive to profound decreases in brain glucose analogous to those that would initiate the counterregulatory response to hypoglycemia in vivo (e.g., 0.1 mmol/l) (12) or whether they are capable of sensing the small physiological changes in glucose concentration associated with daily glucose homeostasis (e.g., from 2.5 to 1 or 5 mmol/l) (10,12). As indicated in Fig. 4, APF (Fig. 4A), input resistance (B), and K<sub>ATP</sub> channel currents (C) show dose-dependent responses to changes

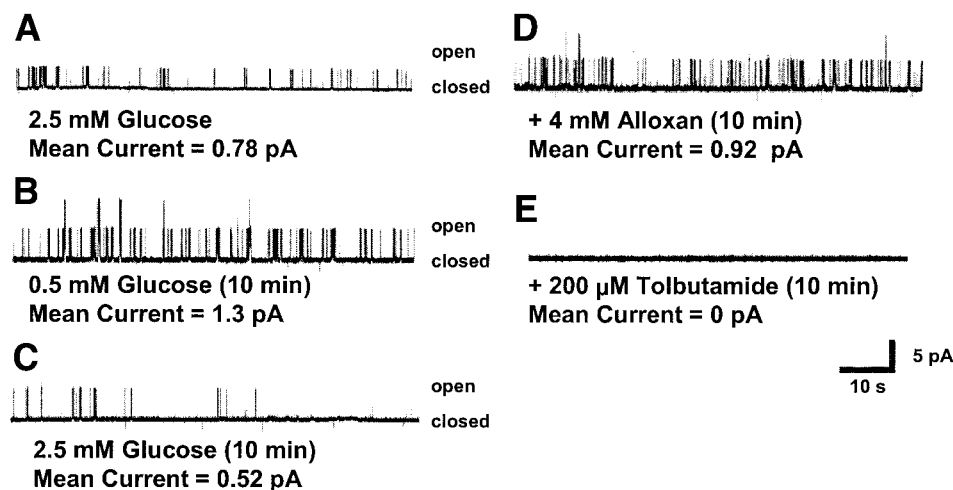


**FIG. 3.** Decreasing glucose from 2.5 to 0.5 mmol/l or adding the glucokinase inhibitor alloxan reversibly increases K<sub>ATP</sub> single-channel currents in a cell-attached recording from an isolated VMH glucose-excited neuron. K<sub>ATP</sub> currents are inhibited by tolbutamide.

in extracellular glucose within the physiological range. APF and input resistance were well fit by a rectangular hyperbole, with the greatest glucose sensitivity (steepest slope) occurring  $<2$  mmol/l (19). Thus, ARC glucose-excited neurons may be capable of sensing meal-induced fluctuations in extracellular glucose levels (10,12). In addition to sensing glucose, we hypothesized that ARC glucose-excited neurons would also be sensitive to leptin and insulin. However, ARC glucose-excited neurons are not sensitive to 10 nmol/l leptin in the presence of either 2.5 ( $n = 7$ ) (Fig. 5A) or 0.1 mmol/l ( $n = 5$ ) (not shown) glucose. This is in sharp contrast to VMN glucose-excited neurons, which are inhibited by 10 nmol/l leptin in the presence of 2.5 mmol/l glucose ( $n = 4$ ) (Fig. 5B). In agreement with Spanswick et al. (8), the effect of leptin on VMN neurons is blocked by tolbutamide, indicating that leptin inhibits VMN glucose-excited neurons by opening the  $K_{ATP}$  channel ( $n = 1$ ) (Fig. 5B, bottom trace). Insulin modulates ARC glucose-excited neurons in a glucose-dependent manner. We previously showed that insulin opened the  $K_{ATP}$  channel and inhibited ARC glucose-excited neurons in 10 mmol/l glucose (9). However, in this study, seven of eight ARC glucose-excited neurons were not affected by insulin (100 or 300 nmol/l) in the presence of 2.5 mmol/l glucose, whereas the eighth neuron actually depolarized and increased its APF by 180%. On the other hand, four of five ARC glucose-excited neurons that were exposed to the same level of insulin in the presence of 0.1 mmol/l glucose transiently depolarized by  $3 \pm 1$  mV and increased their APF by  $215 \pm 115\%$  ( $P = 0.05$ , Students paired  $t$  test) (Fig. 6). Three of these latter four neurons showed no response to insulin in the presence of 2.5 mmol/l glucose (the fourth was not tested in 2.5 mmol/l glucose).

POMC neurons in the lateral ARC (where we find glucose-excited neurons) have both NPY receptors and melanocortin autoreceptors. Thus, we postulated that ARC glucose-excited neurons might respond to NPY and  $\alpha$ -MSH, and that they in fact belong to the POMC neuronal population (4,20). Indeed, NPY (100 and 200 nmol/l) (20,21) hyperpolarizes glucose-excited neurons by  $4 \pm 1$  mV and completely prevents them from firing action potentials ( $n = 6$ ) (Fig. 7A, top). This response persists in high- $Mg^{2+}$  ACSF, indicating that NPY acts directly on ARC glucose-excited neurons ( $n = 3$ ) (Fig. 7A, bottom). On the other hand,  $\alpha$ -MSH (600 nmol/l) (21,22) caused a  $3 \pm 1$  mV depolarization and increased APF by  $37 \pm 9\%$  in ARC glucose-excited neurons ( $n = 6$ ) (Fig. 7B, top trace). The response to  $\alpha$ -MSH persisted in the presence of high  $Mg^{2+}$  in two of these neurons (Fig. 7, bottom trace), whereas the response was abolished in two others (not shown). This indicates that  $\alpha$ -MSH can modulate the activity of ARC glucose-excited neurons both directly and presynaptically. Finally, we investigated whether ARC glucose-excited neurons express the POMC peptide, using double-labeled immunocytochemistry. None of the eight glucose-excited neurons that we evaluated showed POMC immunoreactivity, suggesting that at least these glucose-excited neurons were not POMC neurons (Fig. 8).

## DISCUSSION

Mayer and Thomas's (23) glucostatic hypothesis proposes that reduced glucose availability is sensed by the brain as

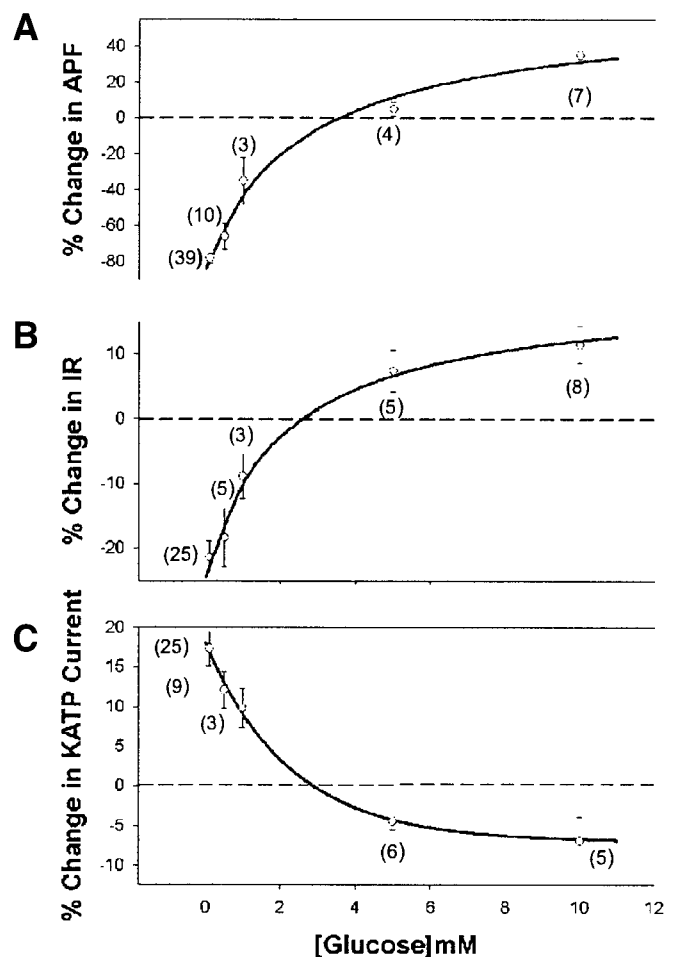
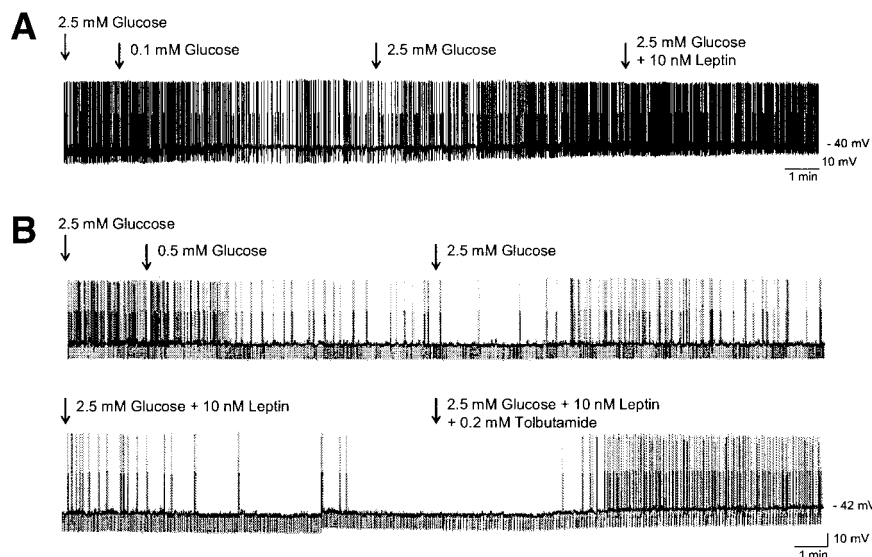


FIG. 4. Dose-dependent response of ARC glucose-excited neurons to physiological alterations in extracellular glucose. Because of variation between neurons, values are expressed as the percent change of APF (A), input resistance (B), and glucose-induced ( $K_{ATP}$  channel) currents (C) compared with 2.5 mmol/l glucose. Data points represent the means  $\pm$  SE, and  $n$  values are in parentheses. The dashed line represents 0% change (by definition, 2.5 mmol/l glucose). A and B: The data fit the following equation for a rectangular hyperbole: % change =  $\{[E_{max} \times (\text{glucose})]/[EC_{50} + (\text{glucose})]\} + i$ , where  $i$  is a constant that does not force the rectangular hyperbole to pass through the origin (ref. 19) and  $EC_{50}$  is the half-maximal effective concentration. For APF,  $E_{max} = 144$  mmol/l and  $EC_{50} = 2.5$  mmol/l. For input resistance,  $E_{max} = 44$  mmol/l and  $EC_{50} = 2.1$  mmol/l. C: The data were initially transformed by adding an integer to give all positive values, as described by Winer (ref. 32). The data were then fit by the following equation for exponential decay (refs. 19 and 32):  $A_c = A_o \times e^{-k[\text{glucose}]}$  with  $A_o = 18$  and  $k = 0.442$ , where  $A_c = K_{ATP}$  current at any concentration of glucose,  $A_o = K_{ATP}$  current at any concentration of glucose,  $e =$  exponential, and  $k =$  decay constant. IR, input resistance.

a trigger for meal initiation. Campfield and Smith (24) later demonstrated that small dips in plasma glucose preceded meal initiation. Although decreased glucose availability may serve as a signal for meal initiation, it is more likely to be a critical signal for integrating autonomic activity and whole-body metabolism (25). The present studies demonstrate that ARC glucose-excited neurons respond in a dose-dependent fashion to physiological changes in extracellular glucose. This supports the hypothesis that the brain is capable of sensing small changes in glucose associated with daily (meal-to-meal) fluctuations in extracellular glucose. Interestingly, ARC glucose-excited neurons are very sensitive to decreases in extracellular glucose levels between 1.5 and 0.5 mmol/l. This raises the



**FIG. 5.** Whole-cell current clamp recordings of spontaneous electrical activity in VMN and ARC glucose-excited neurons. *A:* Leptin (10 nmol/l) in 2.5 mmol/l glucose had no effect on ARC glucose-excited neurons. *B:* Leptin (10 nmol/l) in 2.5 mmol/l glucose decreased membrane potential and APF in a VMN glucose-excited neuron. Tolbutamide reversed this effect (*bottom trace*).

possibility that decreased activity of ARC glucose-excited neurons signals glucose deficit and possibly contributes to meal initiation. This is consistent with the decrease in VMH glucose levels from 1.4 to 0.7 mmol/l seen in the fed versus fasted state (12). ARC glucose-excited neurons show a slight response to increased extracellular glucose levels from 5 to 10 mmol/l. Under physiological conditions, brain glucose levels generally are ~20–30% of plasma levels (10,12). Thus, except in extreme hyperglycemic diabetic conditions, it is unlikely that extracellular brain glucose levels ever exceed 5 mmol/l. However, neuronal processes in the medial ARC do extend into the median eminence, where the blood-brain barrier is permeable (26). Thus, it is possible that ARC glucose-excited neurons are exposed to higher glucose levels than the rest of the brain. Our data showing that they respond to increased glucose levels >5 mmol/l are consistent with this theory. However, it is important to note that this response is small compared with that <2.5 mmol/l glucose.

The mechanism by which glucose-excited neurons detect small changes in extracellular glucose is similar to that in pancreatic  $\beta$ -cells. We showed previously that a subpopulation of isolated VMN glucose-excited neurons, identified by increasing calcium oscillations as extracellular glucose levels increase from 0.5 to 2.5 mmol/l, express glucokinase mRNA (14). The glucokinase inhibitor alloxan (much like low glucose) decreases these calcium oscillations (14). In the present study, we directly evaluated single  $K_{ATP}$  channel currents using the cell-attached patch clamp configuration in cultured VMH glucose-excited neurons. Here, alloxan and 0.5 mmol/l glucose increased  $K_{ATP}$  single-channel currents to a similar degree. This effect was

completely reversible, indicating that it was not caused by any possible neurotoxic effect of alloxan. In isolated neurons, similar results were obtained with three other glucokinase inhibitors that have no neurotoxicity (14). This supports the hypothesis that inhibition of glucokinase in glucose-excited neurons reduces glycolytic flux, and consequently ATP production, causing the  $K_{ATP}$  channel to open (14,15).

Leptin, in 10 mmol/l glucose, opens the  $K_{ATP}$  channel and inhibits VMH glucose-excited neurons (8). However, in the present study of ARC glucose-excited neurons, leptin did not alter APF in the presence of 2.5 or 0.1 mmol/l glucose. This may be caused by differences in extracellular glucose levels used in these studies (i.e., 10 vs. 2.5 or 0.1 mmol/l). However, we and others (8) found that the same concentration of leptin (10 nmol/l) used here opened the  $K_{ATP}$  channel and inhibited VMN glucose-excited neurons in 2.5 mmol/l glucose. It is more likely that this population of ARC glucose-excited neurons, which are located at the dorso-lateral border of the POMC field, do not possess leptin receptors. We have previously shown that only 30% of VMN glucose-excited neurons express mRNA for the long form of the leptin receptor (Obrb) (15). It is possible that the Obrb is heterogeneously distributed among glucose-excited neurons in the ARC as well.

Although leptin had no effect on our ARC glucose-excited neurons, insulin did modulate their activity in a glucose-dependent fashion. We previously showed that insulin in the presence of 10 mmol/l glucose opened the  $K_{ATP}$  channel and inhibited VMH glucose-excited neurons (9). We report here that there is no effect of insulin on ARC glucose-excited neurons in 2.5 mmol/l glucose; however,

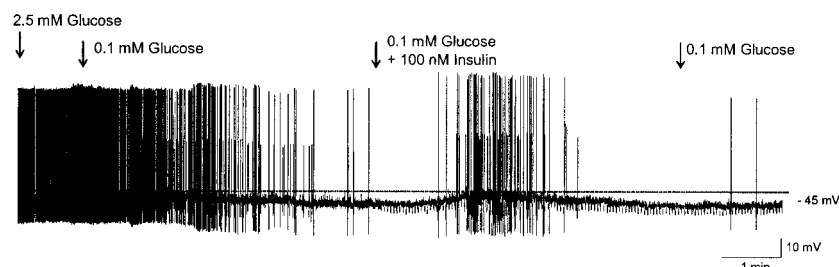


**FIG. 6.** Whole-cell current clamp recordings of spontaneous electrical activity in an ARC glucose-excited neuron. Insulin, in 0.1 mmol/l glucose, caused a transient depolarization and increased APF.

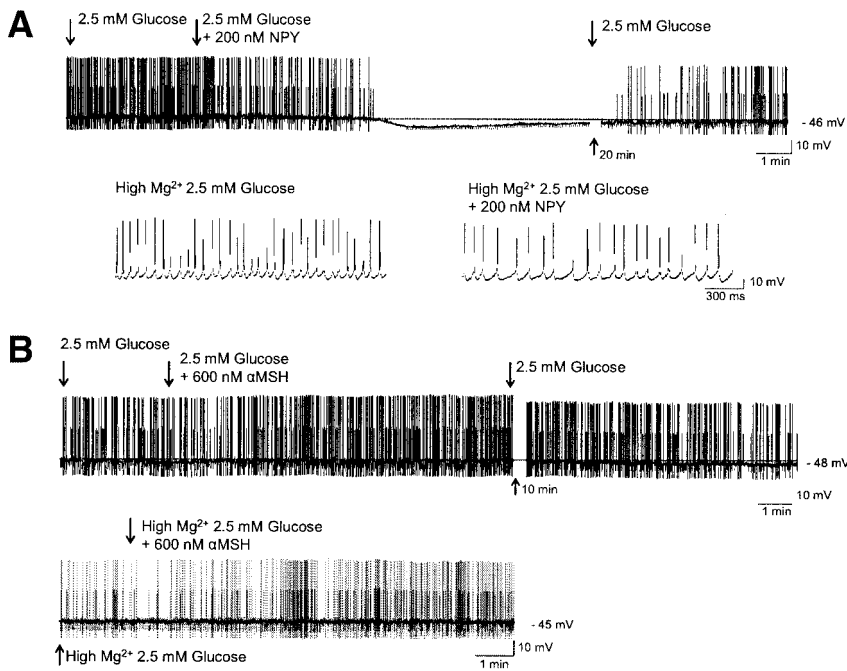


**FIG. 7.** Whole-cell current clamp recordings of spontaneous electrical activity in ARC glucose-excited neurons. *A:* NPY reversibly hyperpolarized and abolished APF in ARC glucose-excited neurons (*top trace*). Although APF was significantly enhanced in the absence of presynaptic input, NPY still reduced APF by 50% in high-Mg<sup>2+</sup> solution (*bottom trace: left, APF = 13.1 Hz in control; right, APF = 6.8 Hz in NPY*). *B:*  $\alpha$ -MSH depolarizes and increases APF in an ARC glucose-excited neuron (*top trace*). This response persists in high-Mg<sup>2+</sup> solution (*bottom trace*).

in the presence of 0.1 mmol/l glucose, insulin actually increases their APF. We hypothesize that there are multiple mechanisms (i.e., excitatory and inhibitory) by which insulin modulates the activity of ARC glucose-excited neurons. In high glucose, the inhibitory effect on the K<sub>ATP</sub> channel may predominate. However, as glucose levels decrease, the K<sub>ATP</sub> channel moves progressively toward the open state. As this occurs, the effect of opening the K<sub>ATP</sub> channel has less of an overall effect on neuronal activity. In 2.5 mmol/l glucose, these opposing effects may be balanced, with the excitatory effect becoming dominant as glucose levels decrease to 0.1 mmol/l. The excitatory effect of insulin may be attributable to increased glucose transport into glucose-excited neurons because we recently found a subpopulation of VMN glucose-excited neurons expressing mRNA coding for both the insulin receptor and the insulin-dependent glucose transporter GLUT4 (15). An interaction between glucose and insulin is not surprising because the brain is never exposed to either insulin or glucose in isolation.

NPY and  $\alpha$ -MSH also modulate the activity of ARC glucose-excited neurons. The observation that NPY inhibits and  $\alpha$ -MSH stimulates ARC glucose-excited neurons is consistent with the opposing roles of these peptides in the regulation of food intake and energy balance (1,2,4,27) as

well as in neuronal excitability (28–30). NPY is a potent orexigen whose expression is upregulated by fasting (1,31). On the other hand  $\alpha$ -MSH produces satiety and increases energy expenditure (4). These data lead to the overall hypothesis that increased activity in glucose-excited neurons reflects adequate energy stores. Thus, in both steady-state glucose levels and in the presence of  $\alpha$ -MSH, these neurons are almost maximally active. However, when glucose levels fall or NPY is present, their activity ceases. The excitatory effect of insulin in 0.1 mmol/l glucose is consistent with this hypothesis. That is, in the presence of insulin, a transient drop in glucose is not as serious an indicator of reduced glucose availability, and therefore glucose-excited neurons are not totally inhibited. It is important to note, though, that the excitatory effect of insulin in low glucose was transient. Thus, even though insulin attenuated the inhibitory effect of low glucose, it did not abolish it, emphasizing that low glucose is a very powerful signal to the brain.

Finally, ARC glucose-excited neurons were not POMC immunoreactive, despite their location in the lateral ARC (4). Most glucose-excited neurons were found intermixed with POMC neurons in the lateral-most aspect of the POMC field. However, because glucose-excited neurons were not distributed through the entire POMC field, it is



**FIG. 8.** Double-labeling immunocytochemistry for lucifer yellow (green) and POMC peptide (red) was not observed in this (or seven other) ARC glucose-excited neurons.

unlikely that all POMC neurons are glucose excited. Furthermore, POMC neurons respond to leptin, whereas ARC glucose-excited neurons did not (20). One technical issue that might have led to a negative result is dialysis of POMC-containing vesicles during standard whole-cell recording. This could prevent us from detecting labeling. However, this is unlikely because of the size of peptide-containing vesicles. Intracellular compartmentalization would also act to prevent dialysis. However, to rule out this possibility, we used perforated patch recording and ruptured the membrane 5 min before concluding the experiment. This allowed lucifer yellow to mark the cell, but it presumably would not allow time for significant dialysis of the large POMC vesicles. Using this technique did not reveal POMC immunoreactivity. Therefore, we conclude that ARC glucose-excited neurons are not of the POMC phenotype, but rather downstream from the POMC and NPY neurons.

In conclusion, ARC glucose-excited neurons dose-dependently increase APF and decrease  $K_{ATP}$  channel currents as glucose levels increase throughout the entire physiological range; however, they are particularly sensitive to decreases in extracellular glucose. Their activity is increased under conditions when glucose levels are adequate (e.g., steady-state to high glucose,  $\alpha$ -MSH, and insulin) and decreased in conditions of glucose deficit (e.g., low glucose and NPY). The fact that they are not POMC immunoreactive, but instead are sensitive to  $\alpha$ -MSH and NPY, suggests that they are downstream from these important neuronal populations. Overall, the data presented herein place ARC glucose-excited neurons in a pivotal position to serve as putative integrators of information regarding peripheral and central energy homeostasis.

#### ACKNOWLEDGMENTS

This study was supported, in part, by National Institutes of Health Grants DK55619 and DK53181 and the Research Service of the Veterans Administration.

We would like to thank Clint Rosenfeld and Dr. Lester Sultatos for their valuable assistance in fitting and interpreting our glucose dose-response data as well as Drs. Hriday Sapru and Vineet Chitravanshi for assistance with subsectioning of the brain slices.

#### REFERENCES

- Broberger C, Hokfelt T: Hypothalamic and vagal neuropeptide circuitries regulating food intake. *Physiol Behav* 74:669–682, 2001
- Williams G, Bing C, Cai XJ, Harrold JA, King PJ, Liu XH: The hypothalamus and the control of energy homeostasis: different circuits, different purposes. *Physiol Behav* 74:683–701, 2001
- Billington CJ, Levine AS: Hypothalamic neuropeptide Y regulation of feeding and energy metabolism. *Curr Opin Neurobiol* 2:847–851, 1992
- Fan W, Boston BA, Kesterson RA, Hrubby VJ, Cone RD: Role of melanocortinergic neurons in feeding and the agouti obesity syndrome. *Nature* 385:165–168, 1997
- Ahima RS, Saper CB, Flier JS, Elmquist JK: Leptin regulation of neuroendocrine systems. *Front Neuroendocrinol* 21:263–307, 2000
- Zhang YH, Lu J, Elmquist JK, Saper CB: Lipopolysaccharide activates specific populations of hypothalamic and brainstem neurons that project to the spinal cord. *J Neurosci* 20:6578–6586, 2000
- Vinuela MC, Larsen PJ: Identification of NPY-induced c-Fos expression in hypothalamic neurones projecting to the dorsal vagal complex and the lower thoracic spinal cord. *J Comp Neurol* 438:286–299, 2001
- Spanswick D, Smith MA, Groppi VE, Logan SD, Ashford MLJ: Leptin inhibits hypothalamic neurons by activation of ATP-sensitive potassium channels. *Nature* 390:521–525, 1997
- Spanswick D, Smith MA, Mirshamsi S, Routh VH, Ashford MLJ: Insulin activates ATP-sensitive  $K^+$  channels in hypothalamic neurons of lean, but not obese rats. *Nat Neurosci* 3:757–758, 2000
- Silver IA, Erecinska M: Glucose-induced intracellular ion changes in sugar-sensitive hypothalamic neurons. *J Neurophysiol* 79:1733–1745, 1998
- McNay EC, Gold PE: Extracellular glucose concentrations in the rat hippocampus measured by zero-net-flux: effects of microdialysis flow rate, strain, and age. *J Neurochem* 72:785–790, 1999
- De Vries MG, Arseneau LM, Lawson ME, Beverly JL: Extracellular glucose in rat ventromedial hypothalamus during acute and recurrent hypoglycemia. *Diabetes* 52:2767–2773, 2003
- Song Z, Levin BE, McArdle JJ, Bakhos N, Routh VH: Convergence of pre- and postsynaptic influences on glucosensing neurons in the ventromedial hypothalamic nucleus. *Diabetes* 50:2673–2681, 2001
- Dunn-Meynell AA, Routh VH, Kang L, Gaspers L, Levin BE: Glucokinase is the likely mediator of glucosensing in both glucose-excited and glucose-inhibited central neurons. *Diabetes* 51:2056–2065, 2002
- Kang L, Routh VH, Kuzhikandathil EV, Gaspers L, Levin BE: Physiological and molecular characteristics of rat hypothalamic ventromedial nucleus glucosensing neurons. *Diabetes* 53:549–559, 2004
- Hentges ST, Nishiyama M, Overstreet LS, Stenzel-Poore M, Williams JT, Low MJ: GABA release from proopiomelanocortin neurons. *J Neurosci* 24:1578–1583, 2004
- Routh VH, McArdle JJ, Levin BE: Phosphorylation modulates the activity of the ATP-sensitive  $K^+$  channel in the ventromedial hypothalamic nucleus. *Brain Res* 778:107–119, 1997
- Dunn-Meynell AA, Rawson NE, Levin BE: Distribution and phenotype of neurons containing the ATP-sensitive  $K^+$  channel in rat brain. *Brain Res* 814:41–54, 1998
- Segel IH: *Enzyme Kinetics*. New York, J. Wiley & Sons, 1975
- Cowley MA, Smart JL, Rubinstein M, Cerdan MG, Diano S, Horvath TL, Cone RD, Low MJ: Leptin activates anorexigenic POMC neurons through a neural network in the arcuate nucleus. *Nature* 411:480–484, 2001
- Fong TM, Van der Ploeg LHT: A melanocortin agonist reduces neuronal firing rate in rat hypothalamic slice. *Neurosci Lett* 283:5–8, 2000
- Lezcano NE, De Barioglio SR, Celis ME:  $\alpha$ MSH changes cyclic AMP levels in rat brain slices by an interaction with the  $D_1$  dopamine receptor. *Peptides* 16:133–137, 1995
- Mayer J, Thomas DW: Regulation of food intake and obesity. *Science* 156:328–337, 1967
- Campfield LA, Smith FJ: Functional coupling between transient declines in blood glucose and feeding behavior: temporal relationships. *Brain Res Bull* 17:427–433, 1986
- Levin BE, Dunn-Meynell AA, Routh VH: Brain glucose sensing and body energy homeostasis: role in obesity and diabetes. *Am J Physiol* 276:R1223–R1231, 1999
- Ganong WF: Circumventricular organs: definition and role in the regulation of endocrine and autonomic function. *Clin Exp Pharm Physiol* 27:422–427, 2000
- Elmquist JK: Hypothalamic pathways underlying the endocrine, autonomic, and behavioral effects of leptin. *Physiol Behav* 74:703–708, 2001
- Cowley MA, Pronchuk N, Fan W, Dinulescu DM, Colmers WF, Cone RD: Integration of NPY AGRP, and melanocortin signals in the hypothalamic paraventricular nucleus: evidence of a cellular basis for the adipostat. *Neuron* 24:155–163, 1999
- Beech DJ: Actions of neurotransmitters and other messengers on  $Ca^{2+}$  channels and  $K^+$  channels in smooth muscle cells. *Pharmacol Ther* 73:91–119, 1997
- Kim CS, Lee SH, Kim RY, Kim BJ, Li SZ, Lee IH, Lee EJ, Lim SK, Bae YS, Lee W, Baik JH: Identification of domains directing specificity of coupling to G-proteins for the melanocortin MC3 and MC4 receptors. *J Biol Chem* 277:31310–31317, 2002
- Levin BE, Dunn-Meynell AA: Dysregulation of arcuate nucleus prepro-neuropeptide Y mRNA in diet-induced obese rats. *Am J Physiol* 272:R1365–R1370, 1997
- Winer BJ: *Statistical Principles in Experimental Design*. 2nd ed. New York, McGraw-Hill, 1962